Published in "Clinical Anatomy doi: 10.1002/ca.21266, 2011"
which should be cited to refer to this work.

An Anatomical Investigation of the Cervicothoracic Ganglion

N. MARCER,[1]* M. BERGMANN,[1] A. KLIE,[2] B. MOOR,[3] AND V. DJONOV[1]

[1]*Institute of Anatomy, Department of Medicine, University of Fribourg, Fribourg, Switzerland*
[2]*Independent Researcher*
[3]*Department of Orthopaedic Surgery, Hôpital Cantonal, Fribourg, Switzerland*

Anatomical variability within the autonomic nervous system has long been accepted. This study evaluated the anatomical variability of the cervicothoracic ganglion (CTG) according to its form and, in addition, provided precise measurements between the CTG and the anterior tubercle of the transverse process of the sixth cervical vertebra (C6TP), the first costovertebral articulation, and the vertebral artery. Forty-two adult cadavers were dissected, 22 male and 20 females. Five main forms of CTG were documented; spindle (31.9%), dumbbell (23.2%), truncated (21.7%), perforated (14.5%), and inverted-L (8.7%). The means for length, width, and thickness of the CTG were 18.5 mm, 8.2 mm, and 4.5 mm, respectively. The dimensions were found to be slightly larger in the males than females and on the left sides as compared to the right. The mean shortest distance between the CTGs and the vertebral artery was found to be 2.8 mm, whilst the mean shortest distances to C6TP was 25.7 mm and to the first costovertebral articulation was 1.7 mm. There is great variability in the morphology of the CTG with five common forms consistently seen. The relation to the vertebral artery may influence the form of the ganglion. Two previously undocumented forms are recorded; the truncated which describes the important juxtaposition of the CTG and the vertebral artery and the perforated which describes the piercing of the ganglion itself by the artery. The findings are considered to be of clinical importance to anesthetists, surgeons, neurosurgeons, and anatomists.

Key words: cervicothoracic ganglion; stellate ganglion; vertebral artery; morphology; truncated; perforated

INTRODUCTION

Anatomically, the sympathetic ganglionic chain in the cervical region is described classically to have three bilaterally-placed ganglia: superior, middle and inferior. Occasionally reference is made to a fourth inconsistent pair of ganglia, the vertebral ganglia lying on the vertebral arteries (Rosse and Gaddum-Rosse, 1997). Usually the inferior cervical ganglion (ICG) is coalesced with the first and sometimes the second thoracic ganglia to form the so-called stellate or cervicothoracic ganglion (CTG) (Singh et al., 2005), although it may include up to the first four thoracic ganglia (Romanes, 1979; Williams and Warwick, 1980; Chung et al., 2002). The transition from the thoracic kyphosis to the cervical lordosis in the adult human creates a marked change in direction of the sympathetic chain which renders the orientation of the CTG virtually anteroposterior along its long axis at this site. The relations of the CTG are usually described as the longus colli muscle and the

*Correspondence to: N. Marcer, Institute of Anatomy, Department of Medicine, University of Fribourg, Fribourg, Switzerland.
E-mail: nicholasmarcer@bluewin.ch

TABLE 1. Summary of the Findings Made by Other Workers

Author	Measurement	*N*	Left	Right	Combined
Slappendel et al. (1995)	Midline of body to center of head of rib 1	8	17.75 mm	19.25 mm	
	Midline of body to center of CTG	8	23.5 mm	24.75 mm	
	Dome of pleura to center of head of rib 1	8	20.63 mm	16.6 mm	
	Dome of pleura to center of CTG	8	21.25 mm	13.33 mm	
Pather et al. (2006)	Length	48	15.1 mm	17.92 mm	16.51 mm
	Width	48	6.45 mm	6.84 mm	6.65 mm
	Shape				
	Spindle	21	14.6%	13.3%	28%
	Dumbbell	20	13.3%	13.3%	26.7%
	Inverted-L	34	26.7%	26.7%	45.3%
Katritsis et al. (1981)[a]	Relation of vertebral level to superior pole of CTG				
	C6-C7	5			6.8%
	C7	20			27.0%
	C7-T1	36			48.6%
	T1	13			17.6%
	Relation of superior pole of CTG to arterial triangle[a]				
	Within	326			75.8%
	Outside	41			9.6%
	Lateral border	63			14.6%
Kiray et al. (2005)					
	Length	12			20.6 mm
	Width	12			8.3 mm
	Thickness	12			3.9 mm
	Relation to vertebral artery				
	Medial	12			68.4%
	Lateral	12			10.5%
	Posterior	12			21.1%

[a]Katritsis et al. (1981) described an arterial triangle formed by the first part of the subclavian inferiorly, the common carotid artery medially and the vertebral artery laterally.

prevertebral fascia on its medial side, the transverse process of C7 and the first rib posteriorly, the vertebral vessels anteriorly, and the superior intercostal artery on its lateral side. Inferiorly, the suprapleural membrane separates the ganglion from the posterior aspect of the cervical pleura (Romanes, 1979; Williams and Warwick, 1980; Rosse and Gaddum-Rosse, 1997).

The CTG sends an array of branches in all directions that prompted early anatomists to name it the stellate ganglion. Fine filaments descend inferiorly to form a plexus on the subclavian artery and its branches whilst larger filaments, including the so-called vertebral nerve, ascend to form a plexus on the vertebral artery (Tubbs et al., 2007). Grey rami communicantes pass laterally or superolaterally to the sixth to eighth cervical ventral rami. A cardiac branch forms the inferior cervical cardiac nerve which passes with the middle cervical cardiac nerve to the deep part of the cardiac plexus (Cho et al., 2005). In a study of the sympathetic contributions to the cardiac plexus, Pather et al. (2004) noted that a cervico-thoracic cardiac ramus arose from the CTG in 84% of cases.

Clinically the importance of the CTG lies in the treatment of sympathetic-mediated disturbances; e.g., chronic regional pain dysfunction (CRPD), tachycardia, and hyperhydrosis. Although numerous approaches have been described, the most common form of treatment involves injecting local anesthetic in relative proximity to the ganglion, either at the C6 or C7 level to produce the so-called stellate ganglion block (SGB) (Hogan et al., 1992; Hempel, 1993; Elias, 2000; Abdi et al., 2004; Feigl et al., 2007). Interestingly, there is a relative paucity of anatomical detail and, in particular, on the morphology of this ganglion in the literature. This is surprising and somewhat disturbing when one considers the potential problems associated with this procedure which range from a simple but transient Horner's syndrome, through severe hypertensive reactions and esophageal puncture, to convulsions or a lethal retropharyngeal hematoma (Kimura et al., 2005; Higa et al., 2006; Narouze et al., 2007; Huntoon, 2010).

During the past 30 years four major studies have documented the shape of the ganglion and its distance from various anatomical structures. Table 1 summarizes the findings of these studies. The shape of the ganglion was documented by Pather et al. (2006) as spindle, dumbbell, or inverted ''L.'' The study utilized 48 cadavers though of these only 17 were adults (the rest being fetal cadavers) and of these only 29 ganglia were measured for length and width with a mean of 16.51 and 6.65 mm, respectively. Kiray et al. (2005) measured 19 ganglia for length, width, and thickness finding a mean of 20.6, 8.3, and 3.9 mm, respectively. They documented the distances between the various ganglia; superior, middle, cervicothoracic, and vertebral on both sides. Furthermore, they measured the relationship between the cervical sympathetic chain and various nearby structures: medial border of longus colli muscle, intervertebral discs of C2-C7 levels, anterior tubercles of the transverse processes of C2-C6, and vertebral artery. They also calculated a midline cervical sympathetic trunk angle between the right and left sides.

Katritsis et al. (1981), with by far the greatest number of specimens at 440, related the position of the superior pole of the CTG with respect to the transverse process of C7 and the head of the first rib. They described an ''arterial triangle'' bordered inferiorly by the first part of the subclavian artery, medially by the common carotid artery, and laterally by the vertebral artery. They related the position of the superior pole of the CTG to this arterial triangle. The distance between the superior pole of the CTG and the origin of the vertebral artery was measured in 139 specimens and found to be between 0 and 25 mm with a mean of 4 mm.

Slappendel et al. (1995) used magnetic resonance imaging to quantify the anatomic variability of the ''stellate ganglion'' in eight healthy patients. They documented the distance between the center of the CTG and the dome of the pleura in the sagittal plane and between the center of the CTG and the midline of the body in the transverse plane.

In addition to the above four works, Hogan and Erickson (1992) performed magnetic resonance imaging of the CTG in nine healthy volunteers. They stated the appearance to be fusiform, triangular or globular and that the ganglion was smaller than reported by dissection studies with a maximal length of just over 1 cm.

MATERIALS AND METHODS

The cervicothoracic ganglia and related structures were dissected on 42 embalmed adult human cadavers (male $n = 22$, female $n = 20$). The mean age was 82 years (age range 59–96 years), with a male mean of 79 years (59–89 years) and female mean of 84 years (63–96 years). The dissections and measurements were performed in the institutes of anatomy at Fribourg, Berne, and Zurich Universities in Switzerland in accordance with the cantonal and national policy and requirements for working with cadaver material. The anterior thoracic wall was opened and the lungs and heart removed by medical students as part of their normal dissection classes. The superficial anterior neck musculature was removed by medical students to expose the anterior throat structures. All deeper dissection to expose the sympathetic chain, the bony landmarks, and the vascular structures in the vicinity of the sympathetic chain was performed by us. The center of the first costovertebral articulation was located by palpation and a pin was then inserted into the joint and the articulation was mobilized manually via the first rib to confirm.

Once the structures were exposed the measurements were made using a Mitutoyu Digimatic Caliper IP67™, Japan. Measurements were made of the length, width, and thickness of the CTG at their greatest points. The length was measured along the long axis of the sympathetic chain, width coronal to that and thickness sagittal to it. Furthermore, the shortest distance from the CTG to the anterior tubercle of the transverse process of C6 vertebra (C6TP), the first costovertebral articulation and to the vertebral artery were also noted. The first costovertebral articulation and C6TP were chosen for measurement as they are easily locatable bony landmarks, the latter being pivotal for several SGB techniques (Hogan and Erickson, 1992; Pather et al., 2004). The vertebral artery is an important structure to avoid in a SGB procedure in case of hemorrhage or the risk of injecting directly into the cerebral blood supply.

RESULTS

Forty-two cadavers were dissected giving a total of 84 cervico-thoracic ganglia. Originally, we began to document the morphology of the ganglia by using the three forms described by Pather et al. (2006). (Fig. 1a–1c). However, it became apparent that, though there is great variability of the ganglia, two other forms were seen quite consistently: a perforated and a truncated form (Fig. 1d and 1e). In the perforated form, the vertebral artery passed directly through the CTG, usually at the superior portion. The gray rami accessed the artery from the posterior aspect as did the filaments that formed the vertebral plexus. In the truncated form, the vertebral artery passed in close proximity to the superior pole of the CTG and created a shortened and flattened form of the ganglion. Often in this case, the rami circled the artery to continue their course.

A true CTG was found in 69 of 84 sides (82%) dissected. The other 15 (18%) were of separate inferior cervical and first thoracic ganglia. The spindle form of ganglion was noted in 22 ganglia (31.9%), the dumbbell in 16 (23.2%), the inverted-L in 6 (8.7%), the perforated in 10 (14.5%), and the truncated in 15 (21.7%). With respect to laterality, the spindle form was found less often on the left side than the right (ratio 9:13), the dumbbell left to right ratio was 7:9, the inverted-L ratio was 4:2, and the truncated 7:8, while the perforated were found in equal numbers of 5:5 (see Table 2 for summary).

Numbers of the different forms of the ganglia varied slightly between male and female cadavers. The perforated form was found in equal numbers of 5:5, respectively, the spindle form accounted for 20.3% of the female ganglia but only 11.6% of the male ganglia. In the female cadavers both the truncated

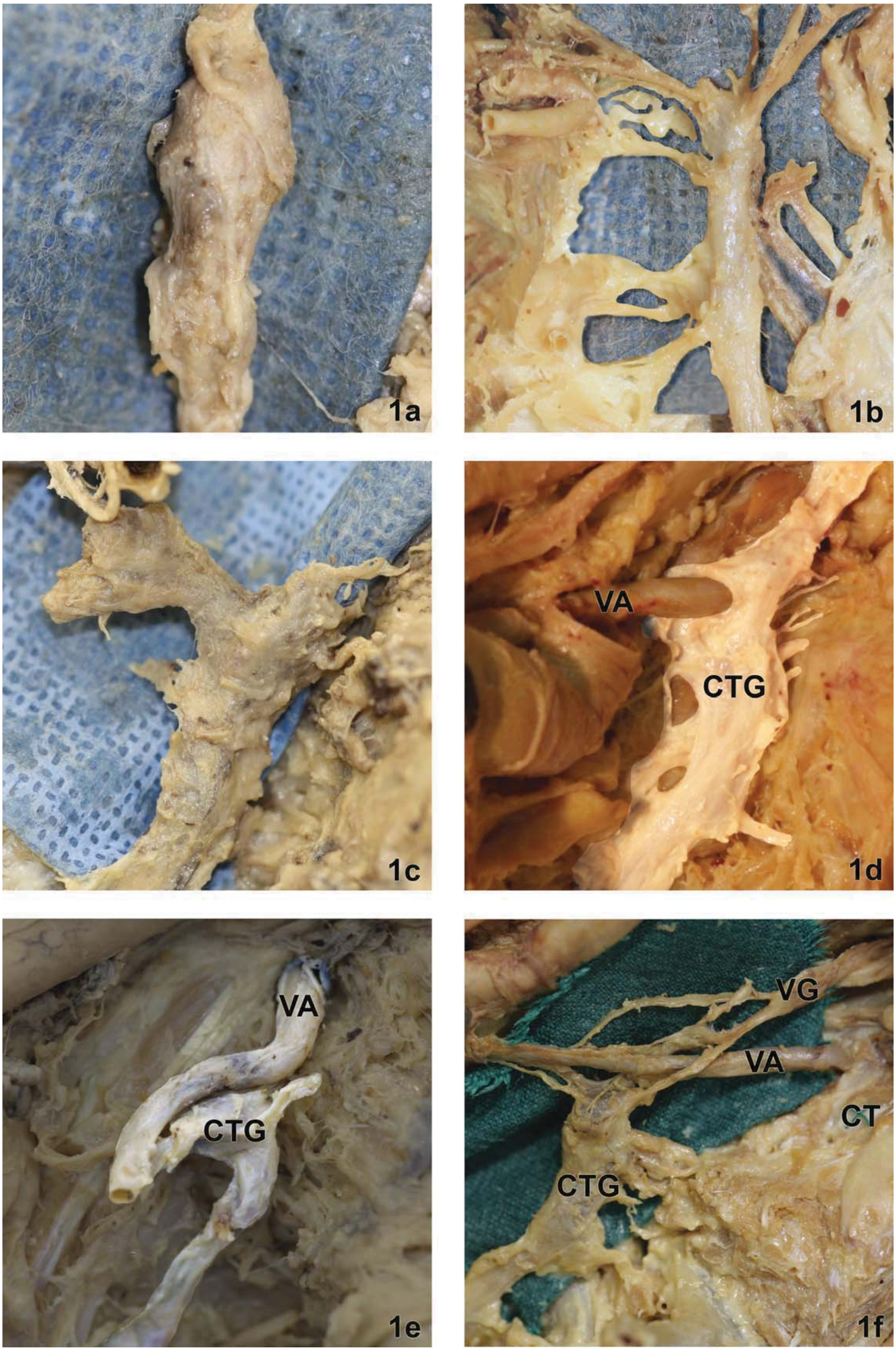

Fig. 1. **a**: Dumbell form. **b**: Spindle form. **c**: Inverted-L form. **d**: Perforated form. CTG, cervicothoracic ganglion; VA, vertebral artery. **e**: Truncated form. CTG, cervicothoracic ganglion; VA, vertebral artery. **f**: Illustrates the presence of a vertebral ganglion. CT, C6TP; CTG, cervicothoracic ganglion; VA, vertebral artery; VG, vertebral ganglion. [Color figure can be viewed in the online issue, which is available at wileyonlinelibrary.com.]

TABLE 2. Summary of CTG Morphology: Number of Ganglia (Percentage)[a]

	Total	Male	Female	Left	Right
Spindle	22 (31.88)	8 (11.59)	14 (20.29)	9 (13.04)	13 (18.84)
Dumbbell	16 (23.19)	10 (14.49)	6 (8.69)	7 (10.14)	9 (13.04)
Inverted-L	6 (8.69)	4 (5.79)	2 (2.89)	4 (5.79)	2 (2.89)
Truncated	15 (21.74)	9 (13.04)	6 (8.69)	7 (10.14)	8 (11.59)
Perforated	10 (14.49)	5 (7.25)	5 (7.25)	5 (7.25)	5 (7.25)

[a]Values in parentheses indicate percentage.

and dumbbell forms were each found present in 8.7% of cases, whereas the same for the males accounted for 13.0% and 14.5%, respectively.

The mean length was 18.50 mm, width 8.17 mm, and thickness of 4.52 mm (Table 3). It was noted that the left ganglia were larger in all dimensions than the right. Slight differences were noted between male and female dimensions with male dimensions being slightly greater in all measurements; male length 19.50 mm, width 8.62 mm, and thickness of 4.94 mm, whereas the female ganglia measured 17.41 mm, 7.67 mm, and 4.06 mm, respectively.

The total mean distance between the CTG and the first costovertebral articulation was found to be 1.72 mm; the mean for the left side was 1.73 mm and the right side 1.70 mm. The mean distance from the CTG to the first costovertebral articulation in the male was 1.83 mm; the mean on the left was 2.55 mm and 1.19 mm on the right, whereas the means for the females was a total of 1.59 mm with 0.81 mm on the left and 2.24 mm on the right.

The mean distance from the CTG to the C6TP was 25.72 mm; the mean for the left side was 26.68 mm and the right side 24.94 mm. The distance measured from the CTG to C6TP in the male cadavers was 27.15 mm and 24.22 mm in the females.

The mean distance from the CTG to the vertebral artery was found to be 2.78 mm with a male mean of 2.99 mm and a female mean of 2.57 mm. The mean distance on the left was measured as 2.69 mm and on the right as 2.88 mm (see Table 3 for summary). Dimensions and distance measurements for the different morphological forms of ganglia are provided in Table 4.

DISCUSSION

A number of works have described the various forms of the CTG and many refer to the dumbbell form. A problem arises in the precise definition of where the dumbbell form ends and two separate ganglia begin. A literature review indicated wide variability in the prevalence of CTG ranging from 37.7% to an unstated presumed 100%. Table 5 summarizes these works.

Pather et al. (2006) was the only research group to describe one of the forms as inverted-L, while others described still further forms as triangular or globular. Although we found instances of all these forms we decided to include the ‘‘truncated’’ form which covered some of these various forms but further indicated that they were ‘‘foreshortened or altered’’ by the position of the vertebral artery. Since Pather et al. (2006) only used three forms of classification, there is undoubtedly a difference between our findings.

Pather et al. (2006) noted that the inverted-L was the most common form 45.3%, followed by spindle at 28%, and dumbbell at 26.7%. Our findings revealed the spindle form to be the most common at

TABLE 3. Summary of Mean Measurements in mm ± SD[a]

	Total, $n = 69$	Male, $n = 36$	Female, $n = 33$	Left, $n = 32$	Right, n = 37
Length	18.50 ± 4.38	19.50 ± 4.21	17.41 ± 4.37	19.02 ± 4.31	18.05 ± 4.46
Width	8.17 ± 2.32	8.62 ± 2.34	7.67 ± 2.23	9.19 ± 2.37	7.28 ± 1.89
Thickness	4.52 ± 1.41	4.94 ± 1.47	4.06 ± 1.19	4.61 ± 1.45	4.44 ± 1.38
1st C/V joint	1.72 ± 2.80	1.83 ± 3.22	1.59 ± 2.29	1.73 ± 3.35	1.70 ±2.26
Vertebral artery	2.78± 4.48	2.99 ± 5.48	2.57 ± 3.10	2.69 ± 4.92	2.88 ± 4.12
TP of C6	25.72 ± 5.63	27.15 ± 5.40	24.22 ± 5.56	26.68 ± 5.73	24.94 ± 5.50

[a]*P*-values: length, 0.103; width, 0.528; thickness, 0.595.

TABLE 4. Summary of Mean Measurements of Different Morphology of CTG in mm ± SD

	Length	Width	Thickness	1st C/V joint	Vertebral artery	TP of C6
Spindle	16.48 ± 4.14	8.43 ± 2.18	4.33 ± 1.56	2.53 ± 2.70	2.67 ± 3.92	25.68 ± 6.64
Dumbbell	19.21 ± 3.83	8.12 ± 2.06	5.10 ± 1.55	0.59 ± 1.69	3.93 ± 5.85	25.69 ± 4.26
Inverted-l	23.07 ± 4.78	7.69 ± 2.74	4.22 ± 1.13	3.44 ± 5.92	4.60 ± 5.46	28.48 ± 5.67
Truncated	17.92 ± 4.02	7.88 ± 2.79	4.68 ± 1.26	0.87 ± 1.87	2.88 ± 4.29	25.71 ± 4.65
Perforated	19.94 ± 3.91	8.38 ± 2.38	3.94 ± 0.98	1.96 ± 2.30	0	24.39 ± 6.94

TABLE 5. Incidence of Cervicothoracic Ganglion

Incidence	Author	Year
83%	Perlow and Vehe	1935
80%	Pick and Sheehan	1946
82%	Jamieson et al.	1952
37%	Becker and Grunt	1957
80%	Jit and Mukerjee	1960
88%	Ellison and Williams	1969
Not stated	Katritsis et al.	1981
Not stated	Groen et al.	1987
84%	Hogan et al.	1992
Not stated	Slappendel et al.	1995
80%	Elias	2000
79%	Kiray et al.	2005
84%	Pather et al.	2006
70%	Ataíde et al.	2008

31.88%, followed by dumbbell 23.19%, truncated 21.74%, perforated 14.49%, and least common was the inverted-L at 8.69%. This discrepancy with the findings of Pather et al. (2006) may be explained by the various other forms cited by other authors being categorized under inverted-L by Pather et al. (2006) as opposed to separate entities. The triangular, tear-drop, globular, and inverted-L described by other authors are most likely to be of those forms because of the proximity to the vertebral artery itself. However, it should be noted that this study used only adult cadavers, whereas Pather et al. (2006) used preserved fetuses in almost two-thirds of their calculations. Development from fetus through child to adult may affect the form of the ganglia but no studies were found that support these possible developmental changes. Interestingly, in another study, Pather et al. (2003) noted that the incidence of CTG was 91% in the fetal specimens as compared to only 69% in the adults which may further indicate a possible change as growth progresses.

Our findings of mean length, width, and thickness differ slightly from that of Kiray et al. (2005) and of the length and width as measured by Pather et al.

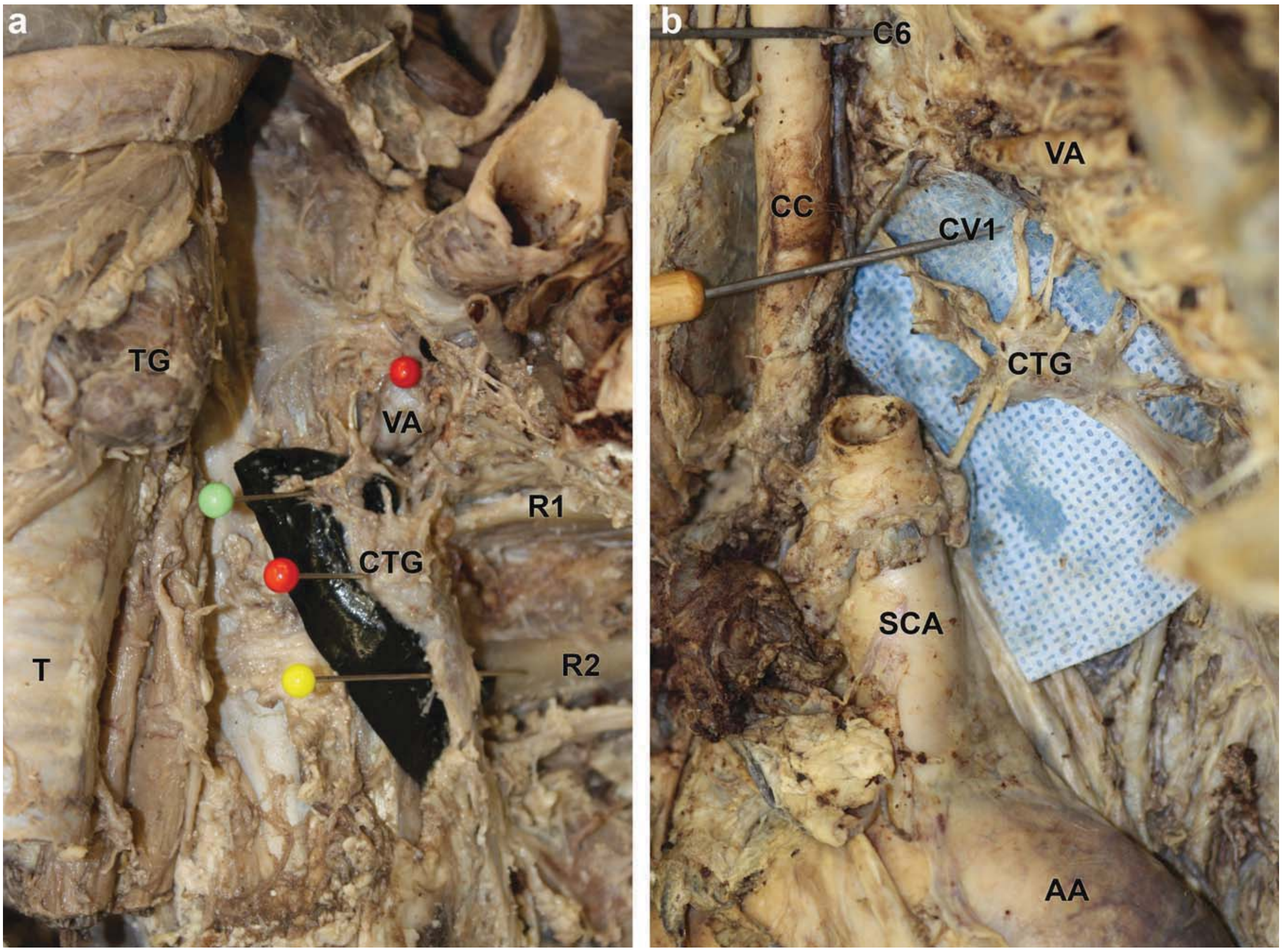

Fig. 2. **a**: Illustrates the relations of the CTG to the ribs. CTG, cervicothoracic ganglion; R1, first rib; R2, second rib; T, trachea; TG, thyroid gland; VA, vertebral artery reflected superiorly. **b:** Illustrates the relations of the CTG to the associated arteries. AA, aortic arch; CC, common carotid artery; CTG, cervicothoracic ganglion; CV1, first costovertebral joint; C6 C6TP; SCA, subclavian artery; VA, vertebral artery reflected superolaterally. [Color figure can be viewed in the online issue, which is available at wileyonlinelibrary.com.]

(2006) though neither of those studies makes mention of the gender of the cadavers. A relationship in the average size of the ganglia and the gender was noted, with male ganglia being on average 12.0% longer, 12.4% wider, and 21.7% thicker than those of females. This would be consistent with the relative size differences noted between male and female cadavers in the general population. However, a further size difference was noted due to laterality with those ganglia on the left side being larger than those of the right in all three dimensions measured. A possible explanation for this size difference could be related to their physiological function. The distribution of postganglionic sympathetic cardiac fibers to the ventricles of the heart differs between left and right ganglia (Yanowitz et al., 1966; Cao et al., 2000; Esler and Kaye, 2006; Kreusser et al., 2006), but there are discrepancies in the literature with respect to the roles of the left and right CTG in cardiac function. The left CTG appears to be predominant over the right with respect to their effects on the QT interval. The right CTG, however, has been noted to be predominant with respect to autonomic innervation of the sinus node (Wong, 1997; Fujiki et al., 1999; Song et al., 2009).

One of the greatest areas for discrepancies in the literature with respect to the CTG is its precise anatomical position. It has been placed anywhere from on the neck of the first rib, to the base of the transverse process of C7 and even as distant as the C7-T1 intervertebral disc (Lockhart et al., 1965; Romanes, 1979; Rosse and Gaddum-Rosse, 1997). Katritsis et al. (1981) stated that the superior pole of the CTG was found within an arterial triangle bordered by the subclavian artery inferiorly, the common carotid artery medially, and the vertebral artery laterally in 75.8% of specimens. They further divided the arterial triangle into three portions, superior, middle, and inferior portions, and documented that the superior pole of the CTG when found within the triangle was found in the inferior third in 79.8% of cases. These workers recorded the distance of the superior pole of the CTG to the vertebral artery to be between 0 and 25 mm with a mean of 4 mm. Our findings were of similar values: between 0 and 18.12 mm but with a mean of 2.78 mm. No significant difference was noted between left and right with mean values of 2.69 mm and 2.88 mm, respectively, nor between gender where the measurements for males was 2.99 mm as compared to 2.57 mm in the females. Katritsis et al. (1981) made no mention of arterial anatomical variability and went as far as to state that the course of the vertebral artery is a constant landmark for the identification of the CTG itself. The only other paper to make specific mention of the intimate relationship between the vertebral artery and the CTG was by Perlow and Vehe (1935) (see Fig. 2a and 2b for detail).

Authors have noted great variability in the origin and course of the vertebral artery: from the aortic arch, common carotid artery or from the subclavian artery distal to the thyrocervical trunk or from the trunk itself (Chen et al., 1998; Gluncic et al., 1999; Koenigsberg et al., 2003; Strub et al., 2006). Though rare, the right vertebral artery has been reported as originating as the last branch off the aorta, distal to the left subclavian artery. A number of authors have noted that the left vertebral artery is more likely to be tortuous than the right (Matula et al., 1997; Huntoon, 2010). As such, assuming the vertebral artery is a constant landmark for identification of the CTG is a little too presumptuous, especially when describing it as of surgical significance (Katritsis et al., 1981). Nevertheless, the relationship between the CTG and the vertebral artery is an important one for distribution of post-ganglionic sympathetic fibers to the posterior cerebral vasculature (Mitchell, 1952). All other previous studies appear to have ignored the intimate proximity of the CTG ganglion and the vertebral artery. It is with this thought in mind that we further the thoughts of Katritsis et al. (1981) and we underline the importance to the surgeon of the spindle form which lacks a definite waist as was previously stated by Pather et al. (2006). Any form of intervention in proximity to the CTG must be performed with a possible intimate relationship to the vertebral artery in mind. Furthermore, we propose the recognition of two previously undocumented forms: truncated and perforated. We hope our finding will be of relevance to anesthetists, surgeons, neurosurgeons, and anatomists.

ACKNOWLEDGMENTS

We acknowledge the assistance given by Nadine Gubler, Franz Jungo, Eric Rouiller, Pierre Sprumont and Clemens Weber of Fribourg University; Suzanne Boemke, Kati Hänssgen and Barbara Krieger of Bern University; Magdalena Vich of Zürich University and Natacha Largo-Robertini and Maurice Waldburger of the Hôpital Cantonal, Fribourg.

REFERENCES

Abdi S, Zhou Y, Patel N, Saini B, Nelson J. 2004. A new and easy technique to block the stellate ganglion. Pain Physician 7:327–331.

Ataíde AM, Brandão BR, Pacheco CL, Calheiros DE, Oliveira GJ, Neto BL, Sousa-Rodrigues CF, Olave E. 2008. Estudio Topográfico y Biométrico del Ganglio Cervicotorácico (Ganglio Estrellado). Int J Morphol 26:451–455.

Becker RF, Grunt JA. 1957. The cervical sympathetic ganglia. Anat Rec 127:1–14.

Cao JM, Chen LS, KenKnight BH, Ohara T, Lee MH, Tsai J, Lai WW, Karagueuzian HS, Wolf PL, Fishbein MC, Chen PS. 2000. Nerve sprouting and sudden cardiac death. Circ Res 86:816–821.

Chen CJ, Wang LJ, Wong YC. 1998. Abnormal origin of the vertebral artery from the common carotid artery. AJNR Am J Neuroradiol 19:1414–1416.

Cho HM, Lee DY, Sung SW. 2005. Anatomical variations of rami communicantes in the upper thoracic sympathetic trunk. Eur J Cardiothorac Surg 27:320–324.

Chung IH, Oh CS, Koh KS, Kim HJ, Paik HC, Lee DY. 2002. Anatomic variations of the T2 nerve root (including the nerve of Kuntz) and their implications for sympathectomy. J Thorac Cardiovasc Surg 123:498–501.

Elias M. 2000. Cervical sympathetic and stellate ganglion blocks. Pain Physician 3:294–304.

Ellison JP, Williams TH. 1969. Sympathetic nerve pathways to the human heart, and their variations. Am J Anat 124:149–162.

Esler M, Kaye D. 2006. Sympathetic nervous system neuroplasticity. Hypertension 47:143–144.

Feigl GC, Rosmarin W, Stelzl A, Weninger B, Likar R. 2007. Comparison of different injectate volumes for stellate ganglion block: An anatomic and radiologic study. Reg Anesth Pain Med 32:203–208.

Fujiki A, Masuda A, Inoue H. 1999. Effects of unilateral stellate ganglion block on the spectral characteristics of heart rate variability. Jpn Circ J 63:854–858.

Gluncic V, Ivkic G, Marin D, Percac S. 1999. Anomalous origin of both vertebral arteries. Clin Anat 12:281–284.

Groen GJ, Baljet B, Boekelaar AB, Drukker J. 1987. Branches of the thoracic sympathetic trunk in the human fetus. Anat Embryol 176:401–411.

Hempel V. 1993. Die Stellatumblockade. Anaesthesist 42:119–128.

Higa K, Hirata K, Hirota K, Nitahara K, Shono S. 2006. Retropharyngeal hematoma after stellate ganglion block: Analysis of 27 patients reported in the literature. Anesthesiology 105:1238–1245.

Hogan QH, Erickson SJ. 1992. MR imaging of the stellate ganglion: Normal appearance. AJR Am J Roentgenol 158:655–659.

Hogan QH, Erickson SJ, Haddox JD, Abram SE. 1992. The spread of solutions during stellate ganglion block. Reg Anesth 17:78–83.

Huntoon MA. 2010. The vertebral artery is unlikely to be the sole source of vascular complications occurring during stellate ganglion block. Pain Pract 10:25–30.

Jamieson RW, Smith DB, Anson BJ. 1952. The cervical sympathetic ganglia. Quart Bull NW Univ Med Sch 26:219–227.

Jit I, Mukerjee RN. 1960. Observations on the anatomy of the human thoracic sympathetic chain and its branches: With an anatomical assessment of operations for hypertension. J Anat Soc India 9:55–82.

Katritsis ED, Lykaki-Anastopoulou G, Papadopoulos NJ. 1981. The relations of the superior pole of the stellate ganglion to the vertebral artery. Anat Anz 150:259–263.

Kimura T, Nishiwaki K, Yokota S, Komatsu T, Shimada Y. 2005. Severe hypertension after stellate ganglion block. Br J Anaesth 94:840–842.

Kiray A, Arman C, Naderi S, Güvencer M, Korman E. 2005. Surgical anatomy of the cervical sympathetic trunk. Clin Anat 18:179–185.

Koenigsberg RA, Pereira L, Nair B, McCormick D, Schwartzman R. 2003. Unusual vertebral artery origins: Examples and related pathology. Catheter Cardiovasc Interv 59:244–250.

Kreusser MM, Haass M, Buss SJ, Hardt SE, Gerber SH, Kinscherf R, Katus HA, Backs J. 2006. Injection of nerve growth factor into stellate ganglia improves norepinephrine re-uptake into failing hearts. Hyperternsion 47:209–215.

Lockhart RD, Hamilton GF, Fyfe FW. 1965. Anatomy of the Human Body. 2nd Ed. London: Faber and Faber. p 325.

Matula C, Trattnig S, Tschabitscher M, Day JD, Koos WT. 1997. The course of the prevertebral segment of the vertebral artery: Anatomy and clinical significance. Surg Neurol 48:125–131.

Mitchell GA. 1952. Rostral extremities of the sympathetic trunks. Nature 170:533–534.

Narouze S, Vydyanathan A, Patel N. 2007. Ultrasound-guided stellate ganglion block successfully prevented esophageal puncture. Pain Physician 10:747–752.

Pather N, Partab P, Singh B, Satyapal KS. 2003. The sympathetic contributions to the cardiac plexus. Surg Radiol Anat 25:210–215.

Pather N, Singh B, Partab P, Ramsaroop L, Satyapal KS. 2004. The anatomical rationale for an upper limb sympathetic blockade: Preliminary report. Surg Radiol Anat 26:178–181.

Pather N, Partab P, Singh B, Satyapal KS. 2006. Cervico-thoracic ganglion: Its clinical implications. Clin Anat 19:323–326.

Perlow S, Vehe KL. 1935. Variations in the gross anatomy of the stellate and lumbar sympathetic ganglia. Am J Surg 30:454–458.

Pick J, Sheehan D. 1946. Sympathetic rami in man. J Anat 80:12–20.

Romanes GJ. 1979. Cunningham's Manual of Practical Anatomy. Vol 3. 14th Ed. Oxford: Oxford University Press. p 71–72.

Rosse C, Gaddum-Rosse P. 1997. Hollinshead's Textbook of Anatomy. 5th Ed. Philadelphia, PA: Lippincott-Raven. p 728–729.

Singh B, Ramsaroop L, Partab P, Moodley J, Satyapal KS. 2005. Anatomical variations of the second thoracic ganglion. Surg Radiol Anat 27:119–122.

Slappendel R, Thijssen HO, Crul BJ, Merx JL. 1995. The stellate ganglion in magnetic resonance imaging: A quantification of the anatomic variability. Anesthesiology 83:424–426.

Song JG, Hwang GS, Lee EH, Leem JG, Lee C, Park PH, Shin JW. 2009. Effects of bilateral stellate ganglion block on autonomic cardiovascular regulation. Circ J 73:1909–1913.

Strub WM, Leach JL, Tomsick TA. 2006. Left vertebral artery origin from the thyrocervical trunk: A unique vascular variant. AJNR Am J Neuroradiol 27:1155–1156.

Tubbs RS, Loukas M, Remy AC, Shoja MM, Salter EG, Oakes WJ. 2007. The vertebral nerve revisited. Clin Anat 20:644–647.

Williams PL, Warwick R. 1980. Gray's Anatomy. 36th Ed. Edinburgh: Churchill Livingstone. p 1129–1130.

Wong CW. 1997. Stimulation of left stellate ganglion prolongs Q-T interval in patients with palmar hyperhidrosis. Am J Physiol 273:H1696–H1698.

Yanowitz F, Preston JB, Abildskov JA. 1966. Functional distribution of right and left stellate innervation to the ventricles: production of neurogenic electrocardiographic changes by unilateral alteration of sympathetic tone. Circ Res 18:416–428.